

THEORETICAL APPROACHES TO CLUSTERING AND FINE STRUCTURE IN HEAVIEST ELEMENTS

I. SILIȘTEANU¹, A. ȘANDRU, A. O. SILIȘTEANU, B. POPOVICI, A. NEACȘU

Horia Hulubei Institute of Physics and Nuclear Engineering
RO-077125, Bucharest-Magurele, Romania

Received March 27, 2007

Alpha clustering and fine structure provide unique information on the nuclear-scale structure of the heaviest elements. Recent developments in superheavy element research allow us to formulate a quantitative theory of radioactive decay, within multichannel resonance scattering approach, which is described in this work. The work emphasizes the theory extended to more complex nuclear structure at the limits of stability and treats the emission rates near the resonance threshold. The material covered includes formal considerations of the decay problem, derived from a microscopic formulation, as well as practical computational methods, based on selfconsistent models for nuclear structure and low-energy reaction dynamics. The reliability of the results is demonstrated by a comparison between the decay data with relevant theories and with other approaches. Particular emphasis is given to the resonance spectroscopy with position-sensitive charge particle detectors since high-precision calculation of partial widths of narrow resonances have become available and these resonances can be observed in experiments. A primary goal of this work is to study the α -decay properties of new superheavy nuclides with $Z = 106$ – 118 , under current experimental research.

Key words: superheavy elements, alpha-decay; resonance tunneling; valence nucleons.

PACS numbers: 25.70.Jj; 27.90.+b

1. INTRODUCTION

Recent significant progress in the superheavy element (SHE) research has delivered challenging experimental data. This provides the opportunity to interpret the new experimental results for the location of superheavy nuclei on the basis of new data. One of the important objectives of nuclear theory is the use the data extracted from various nuclear reactions in order to derive conclusions concerning nuclear properties. This involves developing and applying theories and methods of predictions, analysis and interpretation of specific data, with the aim of achieving a deeper understanding of the physical nature of

¹Corresponding author. E-mail: silist@theory.nipne.ro

quantum many body systems. Our purpose in this paper is the determination of a nuclide's "existence" or particle (cluster) stability, its main decay modes and half-life, its ground state mass, or its excited states and their decay.

The only successful methods for the laboratory synthesis of new superheavy elements (SHEs) have been fusion-evaporation reactions using heavy-element targets, heavy projectiles and fast and efficient on-line recoil separators. Such reactions are central now to nuclear physics and many of the involved processes being resonance reactions can be observed and measured in experiments. In these reactions there have been detected channels of decay which matched very well the signature expected for the nuclear decay of a superheavy nucleus. Spontaneous decay (α , fission) of superheavy nuclei into different fragments is observed, α -decay being the dominant process. Usually, the heaviest nuclides decay over long α -decay chains, ending in spontaneous fission. Therefore, in all of the cases the identification of the nuclei was made by means of α - α correlations with known daughter nuclei after implantation into position-sensitive charged particle detectors. The data is obtained from decay studies in connection with in beam experiments by measuring excitation functions, the cross-section as a function of the beam energy, reaction decay energies and partial lifetime.

The stability of SHEs which is strongly connected to the shape and deformation can be studied in terms of two of the most important typical structures (TS) in nuclei which are the clustering and fine structure. The experimental signatures of TS have been traditionally strong for radioactive heavy nuclei and are supported by selective excitation in α -decay and α -transfer reactions, rotational and vibrational spaced energy levels, enhanced transition strengths and intensities, and appreciable emission width for the resonant states above the decay threshold. The measurements of the TS in α -decay may provide a powerful method to extend the energy and spin-parity informations from daughter to parent nuclei with support from theoretical investigations and this may lead to identification of nuclei in long decay chains and determining the excitation energies of the daughter nucleus from decay and in-beam studies.

Progress in obtaining the most complete information on the development of TS from stable to exotic loosely-bound nuclei and from lightest to heaviest nuclei is being made on several fronts:

- 1) Improving the structure models in order to describe essential features and obtain spectroscopic information on a number of nuclei that can then be tested against data extracted from decay and in-beam studies.
- 2) Extending the range of applicability of reaction models by using accurate reaction channels methods (*e.g.*, via additional channels including, deformation, exchange effects, antisymmetrisation, etc.).

- 3) Including microscopic structure information in coupled channel reaction models and treating more carefully of “intermediate” systems that are more or less bound or have mixed composition.

In Section 2 we present the basic formulas for calculating the emission rates in the single channel and many channel cases. In Section 2.1 we stress some of the resonance features of the single channel solution that we shall require for the extension, in Section 2.2 to the resonance solution in many channel case. The resonance solution of systems of coupled equations is obtained by a direct numerical integration using step-by-step methods on computer. Some variants of the Gordon and Numerow methods are found to be most efficient for these problems. Applications are given in Sect. 3 for the α -decay of deformed superheavy elements (SHE). Section 4 compares the our results with the previous ones and data and recent data. Concluding remarks are made in Section 5.

2. AN OUTLINE OF THE THEORY

There are many theoretical works in the literature on α -decay of SHEs but it is rather difficult to decide which theory or what combinations of theories should be used for the most significant interpretation of the experimental data. The first microscopic description of α -decay was an application of of a general theory of nuclear reactions, the R-matrix theory [1, 2]: This, combined with shell model, which was introduced at the same time, opened the possibility of performing microscopic calculations for the nucleon clustering into the α -particle and its subsequent emission [3–5]: The R-matrix width contains the channel radius parameter, which is an arbitrary parameter and often is interpreted as a disadvantage of the theory. To overcome this disadvantage, in the dynamical reaction theories [6, 7]: there have been formulated alternative approximations [8–11]: which are reviewed in [21]: The dominant feature of many reaction processes in which two nuclei collide at low energies to form a compound nucleus, which subsequently disintegrates in a pair of nuclei, is the appearance of resonances [15–17]. The characteristic common to all these approximations is the employments of quasistationary resonance levels and the competition between the different modes of disintegrations. The experimental observation of resonances has a great importance in reactions with heavy ions since when they are sharp they may be interpreted as levels of reaction product and since such connection contributes directly to decay and in-beam studies of nuclear structure. In many cases the experimental result is usually clear to indicate the position of level and its width to derive some conclusions regarding the size of the system or the internal normalization of the wave function if it is adjusted to give the unit flux at an infinite distance.

From a mathematical point of view, the problems of Gamow states defined as eigenstates of the time independent Schrodinger equation with purely outgoing boundary, are very similar to those of the continuum shell model for nucleons [15]. In both cases, the usual quantum mechanical rules for normalizations, orthogonality and completeness have to be extended in order to take into account the bound as well as scattering wave functions in a straightforward manner. The complex eigenvalue solutions of the Schrodinger equation give the positions of the resonance states as well as their lifetimes. A description of the resonance phenomena via complex eigenvalue solutions has the advantage of containing stationary structures as well as dynamic coupling effects.

It is the aim of the present paper to extend the developments [12, 17–19] in order to study the radioactive decay properties of nuclei at the limits of stability.

3. DESCRIPTION OF THE FORMALISM

In the simplest case of α -decay of a single resonance state k into a single decay channel n , the decay width is [13]:

$$\Gamma_n^k = 2\pi \frac{\left| \int_{r_{\min}}^{r_{\max}} I_n^k(r) u_n^0(r) dr \right|^2}{\left| \int_{r_{\min}}^{r_{\max}} I_n^k(r) u_n^k(r) dr \right|^2} \quad (1)$$

where $I_n^k(r)$ is the particle (cluster) formation amplitude (FA) and $u_n^k(r)$ and $u_n^0(r)$ are the solutions of the system of differential equations

$$\left[\frac{\hbar^2}{2m} \left(\frac{d^2}{dr^2} - \frac{l(l+1)}{r^2} \right) - V_n(r) + Q_n \right] u_n^0(r) = 0 \quad (2)$$

$$\left[\frac{\hbar^2}{2m} \left(\frac{d^2}{dr^2} - \frac{l(l+1)}{r^2} \right) - V_n(r) + Q_n \right] u_n^k(r) = I_n^k(r) \quad (3)$$

The radial functions in Eqs. (2) and (3) describe the radial motion of the fragments at large and small separations, respectively by using the reduced mass m , the kinetic energy of emitted particle $Q_n = E - E_D - E_p$, the FA $I_n^k(r)$, and the interaction potential $V(r)$. The FA is the antisymmetrized projection of the parent wave function (WF) $|\Psi_k\rangle$ on the channel WF $|n\rangle = \left[\left[\Phi_D(\eta_1) \Phi_p(\eta_2) Y_{lm}(\hat{r}) \right]_n \right]$:

$$I_n^k(r) = r \left\langle \Psi_k \left| \mathcal{A} \left\{ \left[\left[\Phi_D(\eta_1) \Phi_p(\eta_2) Y_{lm}(\hat{r}) \right]_n \right] \right\} \right. \right\rangle \quad (4)$$

where $\Phi_1(\eta_1)$ and $\Phi_2(\eta_2)$ are the internal (space-spin) wave functions of the fragments, $Y_{lm}(\hat{r})$ is the wave function of the angular motion, \mathcal{A} is the inter-fragment antisymmetrizer, r connects the centers of mass of the fragments, and the symbol $\langle | \rangle$ means integration over the internal coordinates and angular coordinates of relative motion. The potential contains the nuclear, Coulomb, and spin-orbit parts:

$$V_n(r) = \langle n | [V^{nucl.}(r) + V^{Coul.}(r) + V^{so}(r)] | n \rangle \quad (5)$$

The equations (2, 3) are solved with usual boundary conditions for the decay problem:

$$u_n^0(r \rightarrow 0) = 0; \quad u_n^0(r \rightarrow \infty) \rightarrow i/2(k_n/\pi Q_n)^{1/2} \{u_n^{(-)}(r) + S_n u_n^{(+)}\} \quad (6)$$

$$u_n^v(r \rightarrow 0) = 0; \quad u_n^v(r \rightarrow \infty) = 0 \quad (7)$$

where $\hbar k_n = (2mQ_n)^{1/2}$, S_n is the scattering amplitude, $u_n^{(\pm)}(r) = G_n(r) \pm iF_n(r)$ and F_n and G_n are the regular and irregular Coulomb functions. The lower limit in integrals (1) is an arbitrary small radius $r_{\min} > 0$, while the upper limit r_{\max} is close to the first exterior node of $u_n^0(r)$. To avoid the usual ambiguities encountered in formulating the potential for the resonance tunneling of the spherical barrier we iterate directly the nuclear potential in equations of motion [14]. The ‘‘one-body’’ (o.b.) resonance width in the single channel problem can be expressed only with the eigenvalues and eigenfunctions of the system:

$$\Gamma_n^{o.b.} = 2\pi \frac{\left| \int_{r_{\min}}^{r_{\max}} G_n(r) u_n^0(r) dr \right|^2}{\left| \int_{r_{\min}}^{r_{\max}} G_n(r) u_n^{o.b.}(r) dr \right|^2} \quad (8)$$

where $u_n^{o.b.}(r)$ is a solution of Eq. (3) in which $I_n^k(r)$ is merely replaced by $G_n(r)$.

3.1. COUPLED CHANNELS. DEFORMED SYSTEM

The relative motion of the fragments can be strongly influenced by couplings of the relative motion of the fragments to several nuclear intrinsic motions. The usual way to address the effects of coupling between the intrinsic degrees of freedom and relative motion is to numerically solve the coupled channel equations, including all the relevant channels. The total decay width for the multichannel decay of the state k into a set of $\{n\}$ different channels is [15]:

$$\Gamma^k = \sum_n \Gamma_n^k, \quad \text{where:} \quad (9)$$

$$\Gamma_n^k = 2\pi \frac{\left| \int_{r_{\min}}^{r_{\max}} I_n^k(r) u_n^0(r) dr \right|^2}{\left| \int_{r_{\min}}^{r_{\max}} I_n^k(r) u_n^k(r) dr \right|^2}. \quad (10)$$

In Eq. (9) $I_n^k(r)$ is the particle (cluster) formation amplitude (FA) and $u_n^k(r)$ and $u_n^0(r)$ are the solutions of the systems of differential equations

$$\left[\frac{\hbar^2}{2m} \left(\frac{d^2}{dr^2} - \frac{l(l+1)}{r^2} \right) - V_{nn}(r) + Q_n \right] u_n^0(r) + \sum_{m \neq n} V_{nm}(r) u_m^0(r) = 0 \quad (11)$$

$$\left[\frac{\hbar^2}{2m} \left(\frac{d^2}{dr^2} - \frac{l(l+1)}{r^2} \right) - V_{nn}(r) + Q_n \right] u_n^k(r) + \sum_{m \neq n} V_{nm}(r) u_m^k(r) = I_n^k(r) \quad (12)$$

Now, the matrix elements $V_{nm}(r)$ of the interaction potential depends on the radial distance between the fragments and also on nuclear deformations of involved nuclei. The matrix elements of the interaction potential are given by:

$$V_{nm}(r) = \langle n | V^{nucl.}(r) + V^{Coul.}(r) + V^{so}(r) | m \rangle \quad (13)$$

The potential we use is taken as . The nuclear Hamiltonian is generated by changing the radius of the daughter nucleus R_0 to a dynamical operator [16]:

$$R_0 \longrightarrow R_0 + \hat{O} = R_0 + \beta_2 R_D Y_{20} + \beta_4 R_D Y_{40} \quad (14)$$

where β_2 and β_4 being the quadrupole and hexadecapole deformation parameters. The resulting nuclear coupling matrix elements between states $|n\rangle = |I0\rangle$ and $|m\rangle = |I'0\rangle$ are

$$\begin{aligned} V_{nm}^{nucl.}(r) &= \langle I0 | V^{nucl.}(r, \hat{O}) | I'0 \rangle - \delta_{nm} V_0^{nucl.}(r) = \\ &= \langle \alpha | I0 | \alpha \rangle \langle \alpha | I'0 \rangle V^{nucl.}(r, \lambda_\alpha) - \delta_{nm} V_0^{nucl.}(r); \end{aligned} \quad (15)$$

$$\hat{O}_{II'} = \left[\frac{5(2I+1)(2I'+1)}{4\pi} \right]^{1/2} \beta_2 R_D (C_{000}^{I2I'})^2 \quad (16)$$

$$+ \left[\frac{9(2I+1)(2I'+1)}{4\pi} \right]^{1/2} \beta_4 R_D (C_{000}^{I4I'})^2. \quad (17)$$

Similarly, the Coulomb matrix elements are then given by

$$\begin{aligned}
V_{nm}^{Coul.}(r) = & \frac{3Z_D Z_p R_D^2}{5r^3} \left[\frac{5(2I+1)(2I'+1)}{4\pi} \right]^{1/2} \left(\beta_2 + \frac{2}{7}(5/\pi)^{1/2} \beta_2^2 \right) (C_{000}^{I2I'})^2 + \\
& + \frac{3Z_D Z_p R_D^2}{9r^5} \left[\frac{9(2I+1)(2I'+1)}{4\pi} \right]^{1/2} \left(\beta_4 + \frac{9}{7} \beta_2^2 \right) (C_{000}^{I4I'})^2.
\end{aligned} \tag{18}$$

In the case in which all exit channels are open the boundary conditions should be:

$$\begin{aligned}
u_n^0(r \rightarrow 0) = 0; \\
u_n^0(r \rightarrow \infty) \rightarrow i/2(k_n/\pi Q_n)^{1/2} \{ \delta_{nm} \exp[-i(k_n - l\pi/2)] - S_{nm} \exp[i(k_n r - l\pi/2)] \}
\end{aligned} \tag{19}$$

$$u_n^v(r \rightarrow 0) = 0; \quad u_n^v(r \rightarrow \infty) = 0 \tag{20}$$

where S_{nm} is the scattering matrix. The solutions $u_n^0(r)$ may be matched to the boundary conditions at two values of r large enough so the terms V_{nm} are negligible. A special type of eigenvalue solution will be considered here for which the behavior of solution in each separate channel is similar to that of G_n in the one channel problem.

4. MODEL ESTIMATES FOR THE α -CLUSTER FORMATION AMPLITUDE

For the α -formation amplitude we employ the microscopic shell model wave functions. This method has been initiated [3, 4], for the harmonic oscillator s.p. wave functions and extended to Woods-Saxon wave functions[11, 17, 18]. Following [17] we use two kinds of FAs: one-body resonance amplitude that results in Breit procedure and the shell model FAs given on the basis of shell model s.p. wave functions [20, 19]. In the first case we obtain the asymptotic formation amplitude $I_n^{o.b.}(r) \cong G_n(r)$ and from Eq. (8) $\Gamma_n^{o.b.}$. In the second case using in Eq. (4) shell model w.f. $|\Psi_k\rangle = \det \|\psi_{nlj}(r_i)\|$ where $i = 1, A$ and $|\Phi_D\rangle = \det \|\psi_{nlj}(r_i)\|$ where $i = 1, A - 4$. one obtains a shell model estimation of formation amplitude $I_n^k(r)$ and from Eq. (1) a shell model width Γ_n^k . The CFA is related to the amplitude of reduced width [17]

$$\gamma_n^k(r) = (\hbar^2/2mr)^{1/2} I_n^k(r). \tag{21}$$

The spectroscopic factor is simply defined as

$$S_n^k = \Gamma_n^k / \Gamma_n^{o.b.} = T_n^{o.b.} / T_n^k \tag{22}$$

is a measure of the contribution of shell effects, finite sizes of nucleons and α -particle which are neglected in the one body approximation where α is a

pointlike particle. The inverse of decay reactions and transfer cluster reactions provide similar information [21, 12].

5. DECAY SPECTROSCOPY

As nuclei move further from β stability on the proton rich side, their binding energy rapidly decreases, do to increasing Coulomb repulsion and reaction Q -values, which leads to major difficulties in their production and also in study of decay properties. The relatively large Q -values cause high excitations in nuclear systems involved and open up many competing decay channels favoring the nuclei closer to stability. Damping these excitations can be very crucial for nuclei produced near the limit of proton stability. Very weak reaction channels can be studied by using the resonant particle spectroscopy (RPS) method [22], and the so called recoil decay tagging (RDT) method [23]. Using these methods in studies of long α -chains of isotopes far of stability, make possible to access the basic nuclear-ground state properties: their masses, lifetimes, energy levels, spins, moments and sizes. The classical fission barriers of the heaviest elements with $Z > 100$ approaches zero because of the large Coulomb energy. However, a series of measurements established that the elements with Z up to 118 are sufficiently bound against fission to preferentially decay by α -emission. A large shell correction energy leads to additional binding and, hence, create sizable fission barrier of up to 8 MeV [24]. The α - SF competing channels have been observed [25–28] in SHEs. Spectroscopic studies of heaviest nuclei close to proton drip-line are particularly interesting. First, because the structure of these nuclei differs strongly from that of other nuclei. Second, the lower levels of these nuclei are inevitably near the proton emission thresholds and the proton and α -decay channels are effectively, the only open ones. Third, spectroscopic studies of long chains of isotopes extending far of stability, make possible to access the basic nuclear-ground state properties of new SHEs.

6. RESULTS FOR THE ELEMENTS 118 AND 116

Experimentally, there is evidence for α -clustering and fine structure (deformation) in SHEs. Aiming at confirmation of a part of recent results [29] for the decay chain of $^{294}118$ and $^{290-291}116$ we estimate the α -decay rates using the shell model formation and resonance reaction amplitudes given by selfconsistent models for nuclear structure and low-energy dynamics. For calculating T_α and S_α we use the s.p. shell model states [19, 20] shown in Figs. 1–2, (protons: $1i_{13/2}$, $2f_{7/2}$, $3p_{3/2}$, neutrons: $2g_{7/2}$, $3d_{5/2}$, $3d_{5/2}$), the deformation parameters [43],

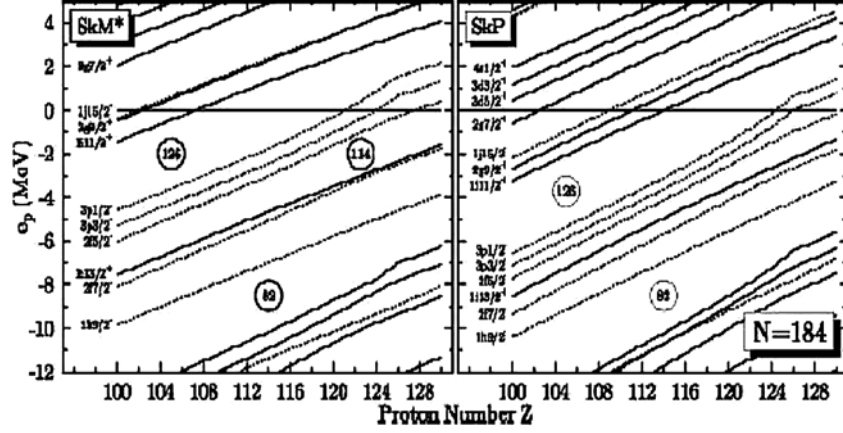


Fig. 1 – Single-proton Fermi levels of the parent and daughter nuclides with $Z = 118-106$ used in (Eq. 4) for calculating the shell-model overlap integrals $I_n^k(r)$. Single-proton levels isotopes are obtained [20] in the RMF approach for $160 \leq N \leq 190$ with NL3 (left) and NL-Z2 no linear parameterizations.

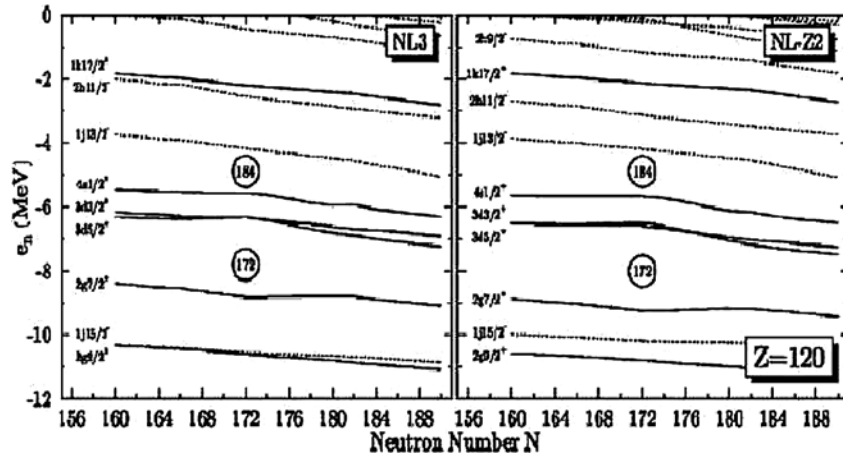


Fig. 2 – Single-neutron Fermi levels of the parent and daughter nuclides [20] used in calculating the overlap integrals $I_n^k(r)$ (Eq. 4) for the nuclides with $Z = 118-106$. The levels for $N = 184$ isotones with $110 < Z < 130$, are obtained with Skyrme-Hartree-Fock model with SKN(left) and SKP effective interactions. Positive (negative) parity levels are indicated by solid (dashed) lines and by their spherical labels (nlj). In both cases the nucleus $Z = 126$ is proton unbound.

the measured [29] $E_\alpha^{\text{exp.}}$ for $^{294}118$, $^{290}116$, $^{286}114$ and calculated ones [30–34] for $^{282}112$ Fig. 3 shows [29] the three α -chains originated from the even-even isotope $^{294}118$ ($E_\alpha = 11.65 \pm 0.06$ MeV, $T_\alpha = 0.89^{+1.70}_{-0.31}$ ms) produced in the 3n-evaporation channel of the $^{249}\text{Cf} + ^{48}\text{Ca}$ reaction with a maximum cross section

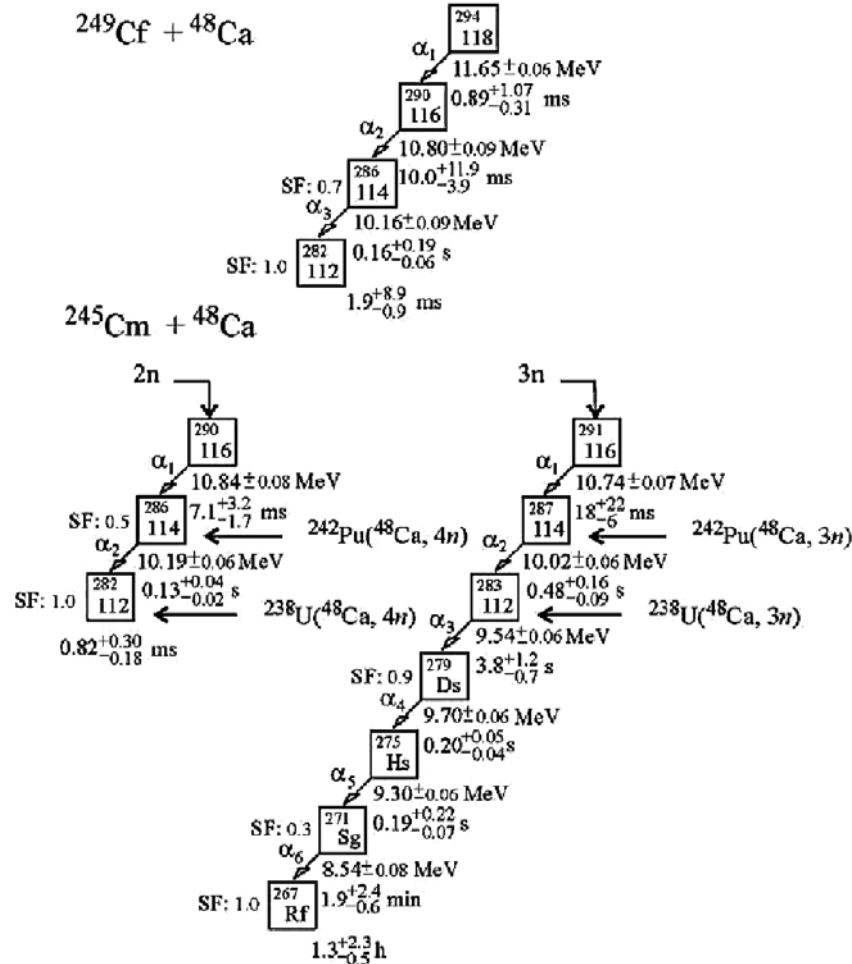


Fig. 3 – Time sequences in the decay α -chains of $^{294}\text{118}$, $^{290}\text{116}$ and $^{291}\text{116}$ observed in the $^{249}\text{Cf} + ^{48}\text{Ca}$ and $^{245}\text{Cm} + ^{48}\text{Ca}$ reactions [29]. The average measured α -particle energies, half-lives, and SF branching ratios of the observed nuclei are shown separately.

of $0.5^{+1.6}_{-0.3}$ pb. Our results are shown in Tables 1–3 and Figs. 4–6. For $^{294}\text{118}$, $^{290}\text{116}$ and $^{286}\text{114}$ we can observe a reasonable agreement with estimates [29]. Also for branching ratios α/SF for $^{286}\text{114}$ and $^{282}\text{112}$ nuclei we observe agreement with data. For Q_α estimates [36–39], the α -channel of $^{282}\text{112}$ practically disappears. The difference in the magnitude of the half-lives between present and previous predictions [44–51], indicate the strong influence of the proton shell at $Z \geq 118$. Theoretical results for the all observed alpha channels are given in Tables 1–3 and are pictured in Figs. 4–6. The calculated α -half-lives being much shorter than the expected fission half-lives are of physical

significance and interest. In most cases our α -half-time estimates are in excellent accord to the existing data and differ from the empirical predictions given by the Viola-Seaborg formula. In the most cases, the decay rates predicted agree well with the measured data. Systematic calculations of spectroscopic properties of SHEs has become feasible, as has been shown on the example of ground states of $^{294}118$ and its α -descendants. The accord to experiment supports the basic correctness of our unified picture for heavy-ion and α -resonances and gives us some guaranty for reasonable predictions to the nuclides with $Z > 114$ just above the magic shell $Z = 114$ and $N = 184$.

Table 1

Decay properties of nuclei produced by Yu. Ts. Oganessian *et al.* [29]

Nuclide	Decay mode	Q_α [MeV]	$T_{1/2}^\alpha$ s		$T_{1/2}^\alpha$ s		S_n^k
			Empiric estimates ^a		Microscopic calculations		
			Ref. [29] Q_α	This work $Q_\alpha + E_{scr}$	Shell model ^b $Q_\alpha + E_{scr}$	Superfl. model ^c $Q_\alpha + E_{scr}$	
$^{294}118$	α	11.81 ± 0.07	$0.89^{+1.07}_{-0.31}$ ms	$0.48^{+0.21}_{-0.15}$ ms	$0.72^{+1.98}_{-0.27}$ ms	$.13^{+49}_{-35}$ ms	$.410^{-3}$
$^{290}116$	α	10.95 ± 0.09	$7.1^{+3.2}_{-1.7}$ ms	$15.15^{+10.50}_{-6.14}$ ms	21^{+16}_8 ms	$2.68^{+1.83}_{-1.08}$ ms	$.210^{-3}$
$^{286}114$	α	10.18 ± 0.09	$0.13^{+0.04}_{-0.02}$ s	$0.40^{+0.31}_{-0.13}$ s	$0.28^{+0.17}_{-0.13}$ s	$0.02^{+0.01}_{-0.01}$ s	$.110^{-3}$
$^{282}112$	α, SF	10.25 ± 0.25^d		$60.49^{+231.90}_{-47.25}$ ms	$40.8^{+154.2}_{-31.92}$ ms	$3.23^{+11.73}_{-2.49}$ ms	$.510^{-3}$

^a Viola-Seaborg formula [40] with parameters [41, 42].^b Shell-model formation amplitude [5, 17].^c Superfluid model formation amplitude [35].^d The limit values include all the predictions: [30–34].

Table 2

Decay properties of nuclei produced by Yu. Ts. Oganessian *et al.* [29]

Nuclide	Decay mode	Q_α [MeV]	$T_{1/2}^\alpha$ s		$T_{1/2}^\alpha$ s		S_n^k
			Empiric estimates ^a		Microscopic calculations		
			Ref. [29] Q_α	This work $Q_\alpha + E_{scr}$	Shell model ^b $Q_\alpha + E_{scr}$	Superfl. model ^c $Q_\alpha + E_{scr}$	
$^{290}116$	α	$11.00 \pm .08$	$7.1^{+3.2}_{-1.7}$ ms	$11.34^{+6.7}_{-4.18}$ ms	$12.70^{+6.9}_{-10.4}$ ms	$12.34^{+7.0}_{-4.4}$ ms	0.20
$^{286}114$	α, SF	$10.33 \pm .06$	$.13^{+0.04}_{-0.02}$ s	$.15^{+0.07}_{-0.04}$ ms	$.14^{+0.17}_{-0.01}$ ms	$.10^{+0.05}_{-0.03}$ ms	0.17

^a Viola-Seaborg formula [40] with parameters [41, 42].^b Shell-model formation amplitude [5, 17].^c Superfluid model formation amplitude [35].

Table 3

Decay properties of nuclei produced by Yu. Ts. Oganessian *et al.* [29]

Nuclide	Decay mode	Q_α [MeV]	$T_{1/2}^\alpha$ s		$T_{1/2}^\alpha$ s		S_n^k
			Empiric estimates ^a		Microscopic calculations		
			Ref. [29] Q_α	This work $Q_\alpha + E_{scr}$	Shell model ^b $Q_\alpha + E_{scr}$	Superfl. model ^c $Q_\alpha + E_{scr}$	
²⁹¹ 116	α	$10.89 \pm .07$	$18^{+22}_{-6}10^{-3}$	$21^{+11}_{-7}10^{-3}$	$27^{+14}_{-5}10^{-3}$	$1.12^{+5.5}_{-3.6}10^{-3}$	0.9110^{-2}
²⁸⁷ 114	α	$10.16 \pm .06$	$0.48^{+0.16}_{-0.09}$	$0.45^{+0.21}_{-0.14}$	$0.62^{+0.2}_{-0.19}$	$16.18^{+4.23}_{-5.01}10^{-3}$	0.5610^{-2}
²⁸³ 112	α	$9.67 \pm .06$	$3.8^{+1.2}_{-0.2}$	$2.56^{+1.29}_{-0.85}$	$3.95^{+1.85}_{-1.11}$	$59.12^{+18.25}_{-24.02}10^{-3}$	0.3010^{-2}
²⁷⁹ 110	α, SF	$9.84 \pm .06$	$0.2^{+0.05}_{-0.04}$	$0.18^{+0.09}_{-0.16}$	$0.10^{+0.06}_{-0.03}$	$8.17^{+3.76}_{-2.53}10^{-3}$	0.1710^{-2}
²⁷⁵ 108	α	$9.44 \pm .06$	$0.19^{+0.22}_{-0.07}$	$0.56^{+0.29}_{-0.19}$	$0.26^{+0.15}_{-0.08}$	$25.41^{+12.66}_{-8.17}10^{-3}$	0.1910^{-1}
²⁷¹ 106	α, SF	$8.67 \pm .08$	114^{+144}_{-36}	$27.33^{+22.68}_{-12.28}$	68^{+51}_{-22}	$1.373^{+1.119}_{-0.611}$	0.410^{-2}

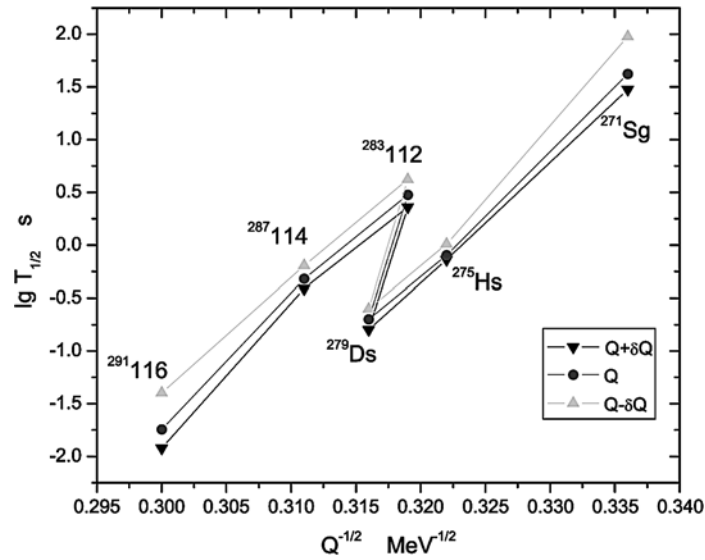
^a Viola-Seaborg formula [40] with parameters [41, 42].^b Shell-model formation amplitude [5, 17].^c Superfluid model formation amplitude [35].

Fig. 4 – The Gamow plot for empirically calculated [29] α -halflives for the element ²⁹¹116 and its α -descendants. The experimental Q_α -values are taken from [29]. Estimates [29] are obtained using the formula [40] with parameters [41, 42].

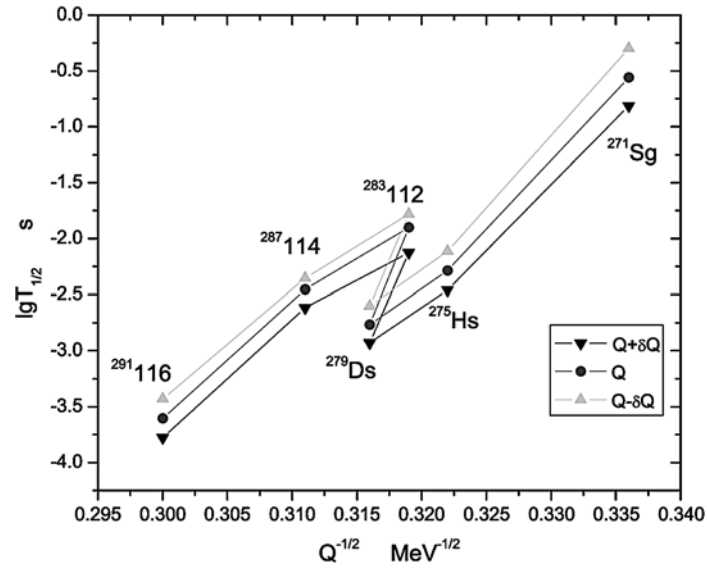


Fig. 5 – The Gamow plot for the half-lives of the nuclide $^{291}116$ and its α -descendants calculated microscopically within this paper.

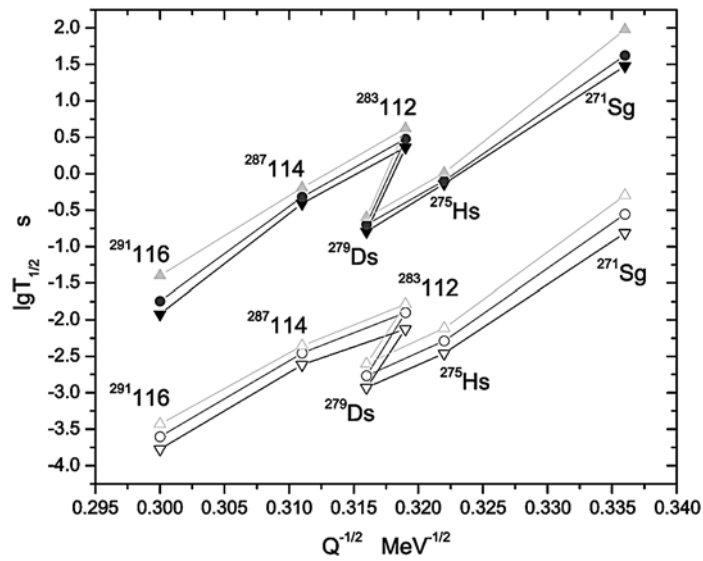


Fig. 6 – The Gamow plot for calculated α -halflives for the element $^{291}116$ and its α -descendants. Full symbols show the results obtained with the shell model overlap integrals (Eq. 4), while the open symbols show the results with the resonance overlap integrals (down triangles correspond to $Q + \delta Q$, up triangles to $Q - \delta Q$ and circles to Q values).

7. SUMMARY AND OUTLOOK

Detailed tests of theoretical models for the nuclear structure and α -decay modes have been performed by wavefunction sensitive quantities. The absolute decay rates of ground and excited states of atomic nucleus are the most important of these quantities. All these probes reveal the crucial details needed to certify a theoretical description of the structure and dynamics of a particular nuclide. Characterized by their lifetime the nuclear decay can be enhanced due to the collective behavior or forbidden by internal selection rules. In this work we calculated in different approximations the α -half-lives of nuclides $^{294}118$, $^{290-291}116$ and their alpha descendants using the measured emission energy, cluster formation amplitude and reaction amplitude for resonance tunneling. Characteristic for these nuclides are long α -chains as well as parallel sequences of α -chains terminating by spontaneous fission. Our study reveals a close connection between particle decay properties, the number of valence nucleons and their single particle structure. The valence nucleon number appears as a dominant controlling factor in evolution of structure and α -decay properties, and therefore, it was possible to devise some observables related to it which describe the systematic and periodic variations in the structure and basic decay properties.

The following conclusions can be drawn from our study:

- 1) The spin-parity and emission energy information can be accurately extended, with support from theoretical investigations, from the daughter to parent (unknown). Thus, the decay chain can be rebuilt from the bottom and this helps to identify new nuclides through their α -decay characteristics and measured α - α , parent-daughter space-time correlations.
- 2) The nuclides just above $Z = 114$ and $N = 184$ are predicted to be prominent α -emitters in this region. The shortest α -half-lives predicted for these nuclides are in the range tens of ms. However, short α -half-lives may prevent direct observation with the current detection methods. The production of these nuclides may become feasible in the future with the use of radioactive beams.
- 3) The structure and nuclear decay properties (emission energies and half-lives) of these groups of elements are a periodic function of the number of valence nucleons. An α -periodicity of this function has been revealed by data and estimated quantities. Therefore, it was possible to deduce the properties of nuclides above $Z = 114$ from what we know in the $Z = 82$ and $Z = 50$ regions by using the symmetry arguments associated to the α -periodicity.

Acknowledgements. We thank Profs. Yu. Ts. Oganessian, V. K. Utyukov, S. Hofmann, G. Münzenberg, W. Scheid, M. Rizea, A. Săndulescu for many stimulating discussions. This work was supported from Contracts: CERES-3/40, 41, 4/218 and CEEX05-D08-10.

REFERENCES

1. T. Teichmann, E. P. Wigner, *Phys. Rev.*, **79**, 30 (1952).
2. R. G. Thomas, *Prog. Theor. Phys.*, **12**, 253 (1954).
3. H. J. Mang, *Phys. Rev.*, **119**, 1069 (1960).
4. H. J. Mang, J. O. Rasmussen, Kgl. Danske Videnskab Selskab, *Mat. Fys. Skifter* 2, **3**, (1962).
5. H. J. Mang, *Ann. Rev. Nucl. Sci.*, **14** (1984).
6. G. Breit, *Encyclopedia of Physics*, Vol. XLI, *Nuclear Reactions II: Theory*, Springer-Verlag, 1959 (ed. S. Flugge).
7. H. Feshbach, *Ann. Phys. 5 (NY)*, **357** (1958).
8. K. Harada, E. A. Rauscher, *Phys. Rev.*, **169**, 818 (1968).
9. S. G. Kadmsky, V. E. Kaletchis, *Yad. Fiz.*, **12**, 70 (1970).
10. J. Schlitter, *Nucl. Phys.*, **A211**, 96 (1973).
11. A. Sandulescu, I. Silişteanu, R. Wuensch, *Nucl. Phys.*, **A305**, 205 (1978).
12. P. E. Hodgson, E. Betak, *Phys. Rep.*, **374**, 89 (2003).
13. I. Silişteanu, W. Scheid, A. Sandulescu, *Nucl. Phys.*, **A679**, 317 (2001).
14. I. Silişteanu, W. Scheid, *Phys. Rev.*, **51**, 2023 (1995).
15. I. Silişteanu, W. Scheid, A. O. Silişteanu, *Rom. Rep. Phys.*, **57**, 4 (2005).
16. K. Hagino, N. Rowley, A. T. Kruppa, *Comp. Phys. Commun.*, **123**, 143 (1999).
17. I. Silişteanu, Preprint E4-80-8, JINR, Dubna (1980).
18. V. I. Furman, S. Holan, G. Stratan, *Nucl. Phys.*, **A 239**, 114 (1975).
19. M. Bender *et al.*, *Phys. Rev.*, **C60**, 034304 (1999).
20. A. T. Kruppa *et al.*, *Phys. Rev.*, **C61**, 034313 (2000).
21. R. G. Lovas *et al.*, *Phys. Rep.*, **294**, 265 (1998).
22. D. Robson, *Nucl. Phys.*, **A204**, 204 (1973).
23. R. S. Simon *et al.*, *Z. Phys.*, **A325**, 197 (1986).
24. P. Reiter *et al.*, *Phys. Rev. Lett.*, **82**, 509 (1999).
25. S. Hofmann *et al.*, *Zeit. Phys.*, **A354**, 229 (1996).
26. S. Hofmann, G. Münzenberg, *Rev. Mod. Phys.*, **72**, 733 (2000).
27. Yu. Ts. Oganessian *et al.*, *Phys. Rev.*, **C69**, 021601 (2004).
28. Yu. Ts. Oganessian *et al.*, *Phys. Rev.*, **C69**, 054607 (2004).
29. Yu. Ts. Oganessian *et al.*, *Phys. Rev.*, **C74**, 044602 (2006).
30. S. Gorieely *et al.*, *Phys. Rev.*, **C66**, 024326 (2002).
31. S. Typel, B. A. Brown, *Phys. Rev.*, **C67**, 034313 (2003).
32. J. F. Berger, D. Hirata, M. Girod, *Acta Phys. Pol.*, **B34**, 1909 (2003).
33. S. Cwiok, P. H. Heenen, W. Nazarewicz, *Nature*, **433**, 705 (2005).
34. M. Warda *et al.*, *Intern. J. Mod. Phys.*, **E15** (in press).
35. F. Barranco, R. A. Broglia, G. F. Bertrech, *Phys. Rev. Lett.*, **60**, 507, (1988).
36. I. Muntian, Z. Patyk, A. Sobiczewski, *Phys. At. Nucl.*, **66**, 1015 (2003).
37. A. Baran *et al.*, *Phys. Rev.*, **C72**, 044310 (2005).
38. Y. K. Gambhir, A. Bhagwat, M. Gupta, *Phys. Rev.*, **C71**, 037301 (2005).
39. M. Bender *et al.*, *Phys. Rev.*, **C61**, 031302 (2000).
40. V. E. Viola, G. T. Seaborg, *J. Inorg. Nucl. Chem.*, **28**, 741 (1966).
41. A. Sobiczewski, Z. Patyk, S. Cwiok, *Phys. Lett.*, **B224**, 1 (1989).
42. Z. Patyk, A. Sobiczewski, *Nucl. Phys.*, **A354**, 229 (1996).
43. P. Möller *et al.*, *At. Data and Nucl. Data Tab.*, **66**, 131 (1997).
44. V. Yu. Denisov, H. Ikezoe, *Phys. Rev.*, **C72**, 064613 (2005).
45. P. Mohr, *Phys. Rev.*, **C73**, 031301 (2006).
46. P. Roy, Chowdhury, C. Samanta, D. N. Basu, *Phys. Rev.*, **C73**, 014612 (2006).

-
47. Chang Xu, Zhongzhou Ren, *Phys. Rev.*, **C74**, 014304 (2006).
 48. Takatoshi Ichikawa *et al.*, *Phys. Rev.*, **C71**, 044608 (2005).
 49. I. Silișteanu *et al.*, *Proc. CSSP-2005 Exotic nuclei and Nuclear/ Particle Astrophysics*, World Scientific, 2006, eds. Stoica, Trache, Tribble, p. 423.
 50. S. G. Nilsson *et al.*, *Phys. Lett.*, **28B**, 458 (1969); *Nucl. Phys.*, **A131** (1969), *Nucl. Phys.*, **A115**, 545 (1968).
 51. E. O. Fiset, J. R. Nix, *Nucl. Phys.*, **A193**, 647 (1972).